

Improved superresolution in coherent optical systems

Amir Shemer, Zeev Zalevsky, David Mendlovic, Emanuel Marom, Javier Garcia, and Pascuala Garcia Martinez

Objects that temporally vary slowly can be superresolved by the use of two synchronized moving masks such as pinholes or gratings. This approach to superresolution allows one to exceed Abbe's limit of resolution. Moreover, under coherent illumination, superresolution requires a certain approximation based on the time averaging of intensity rather than of field distribution. When extensive digital postprocessing can be incorporated into the optical system, a detector array and some postprocessing algorithms can replace the grating that is responsible for information decoding. In this way, no approximation is needed and the synchronization that is necessary when two gratings are used is simplified. Furthermore, we present two novel approaches for overcoming distortions when extensive digital postprocessing cannot be incorporated into the optical system. In the first approach, one of the gratings, in the input or at the output plane, is shifted at half the velocity of the other. In the second approach, various spectral regions are transmitted through the system's aperture to facilitate postprocessing. Experimental results are provided to demonstrate the properties of the proposed methods. © 2001 Optical Society of America

OCIS codes: 100.6640, 170.6920.

1. Introduction

Every optical system can provide only limited spatial resolution. In terms of spatial frequencies, the lens is band limited and functions as a low-pass filter. The numerical aperture and the wavelength determine the cutoff frequency of the system. Thus an extension of the aperture may improve the spatial resolution of the optical system. However, physical extension is costly and is not always possible. The purpose of superresolution is to produce a synthetic enlargement of the aperture without changing the aperture's physical dimensions.

The attempts to obtain effectively larger apertures follow a single principle: They are based on certain *a priori* knowledge about the object. Some examples of such knowledge are that the object be approximately time independent,¹⁻³ polarization independent,⁴ or monofrequency (i.e., wavelength independent).⁵ Recently, these theories were generalized on the

basis of the space-bandwidth product adaptation approach.^{6,7} One of the most appealing approaches for resolving powers that exceed the classic limits is related to temporally restricted objects and is based on two moving gratings.² However, under coherent illumination this approach produces an approximate resolved image.⁸ The approximation is due to time averaging of the intensity instead of the field distribution as required by theory. However, if the expanded synthetic aperture is wider than the spectral bandwidth of the input object (which is also wider than the optical aperture), a good superresolved output can be obtained.

The superresolving approach based on two moving gratings has two major disadvantages: the need for accurate synchronization of two gratings and the need for close contact between the gratings and the input and output planes.

When extensive digital postprocessing can be incorporated into the system, a method based on replacing the second grating with a virtual grating produced electronically and some postprocessing algorithms can be effective.⁹ Figure 1 shows such a system schematically. Furthermore, it was shown in Ref. 3 that, if two Dammann gratings replace the Ronchi gratings, the distortion caused by the non-equal orders will no longer exist.

In Section 2 we give a brief explanation of the main principles behind the time-multiplexing approach.

A. Shemer, Z. Zalevsky, D. Mendlovic (e-mail: mend@eng.tau.ac.il), and E. Marom are with the Department of Physical Electronics, Faculty of Engineering, Tel-Aviv University, 69978 Tel-Aviv, Israel. J. Garcia and P. G. Martinez are with the Departamento d'Optica, Universitat de Valencia, C/Dr. Moliner 50, 46100 Burjassot, Valencia, Spain.

Received 3 October 2000; revised manuscript received 2 May 2001.

0003-6935/01/264688-09\$15.00/0

© 2001 Optical Society of America

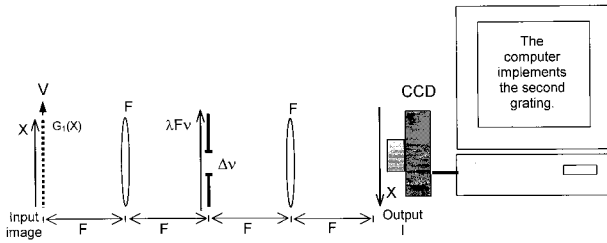


Fig. 1. Optical system for obtaining an increased effective aperture with a physical moving grating at the input plane and a computer-generated virtual grating at the output.

In Section 3 we describe the methods for obtaining accurate coherent superresolution.

2. Operating Principles of Superresolving Optical Systems

A simplified description of the coherent superresolution working principles is based on the system presented in Fig. 1 but with a physical decoding grating instead of a virtual grating. This explanation is necessary for an understanding of ways in which accurate coherent superresolution can be achieved and the way in which the virtual grating technique works.

We consider partitioning the spatial spectrum, $\tilde{U}_{In}(\nu)$, of the object such that it consists of three sequential spatial frequency bands, defined as

$$\begin{aligned} a(\nu) &= [\tilde{U}_{In}(\nu)\text{rect}(\nu/\Delta\nu)], \\ b(\nu) &= [\tilde{U}_{In}(\nu + \nu_0)\text{rect}(\nu/\Delta\nu)], \\ c(\nu) &= [\tilde{U}_{In}(\nu - \nu_0)\text{rect}(\nu/\Delta\nu)], \end{aligned} \quad (1)$$

where $\Delta\nu$ is the cutoff frequency of the band-limited system and ν_0 is the grating's basic frequency [Fig. 2(a)]. In this specific example, the system aperture

is effectively enlarged to three times its actual size. The system can achieve an even wider synthetic aperture than that.

Looking at the overall spatial spectrum, one can see that it can be represented as

$$\begin{aligned} \text{FT}[U_{In}(x)] &= \tilde{U}_{In}(\nu) \\ &= [b(\nu) \otimes \delta(\nu - \nu_0) + a(\nu) \otimes \delta(\nu) \\ &\quad + c(\nu) \otimes \delta(\nu + \nu_0)], \end{aligned} \quad (2)$$

where \otimes denotes the convolution operation. Note that each band has a spatial frequency bandwidth, which is determined by the aperture diameter. The Fourier transform (FT) of the object's intensity is essentially the autocorrelation of the FT of the field distribution,

$$\begin{aligned} \tilde{U}_{In}(\nu) * \tilde{U}_{In}(\nu) &= [c(\nu) * b(\nu)] \otimes \delta(\nu - 2\nu_0) \\ &\quad + [a(\nu) * b(\nu) + c(\nu) * a(\nu)] \\ &\quad \otimes \delta(\nu - \nu_0) + [a(\nu) * a(\nu) \\ &\quad + b(\nu) * b(\nu) + c(\nu) * c(\nu)] \\ &\quad \otimes \delta(\nu) + [b(\nu) * a(\nu) \\ &\quad + a(\nu) * c(\nu)] \otimes \delta(\nu + \nu_0) \\ &\quad + [b(\nu) * c(\nu)] \otimes \delta(\nu + 2\nu_0), \end{aligned} \quad (3)$$

where $*$ denotes the correlation operation. This expression is plotted in Fig. 3(a).

Bearing in mind that Eq. (3) is the spectrum of the desired output image that we want to generate in a superresolution system, let us look at the system in

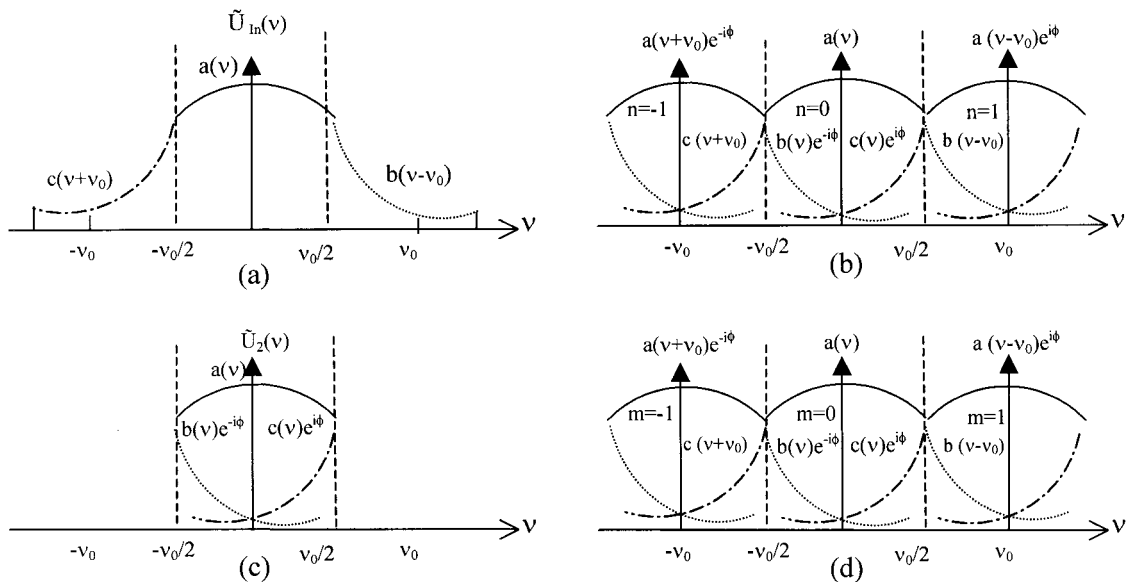


Fig. 2. Main principles of coherent superresolution in the spectral domain: (a) FT of the input, (b) FT of the field distribution after it passes the first grating, (c) FT after it passes the system's limited aperture, (d) FT of the field after it passes the second grating and before time averaging.

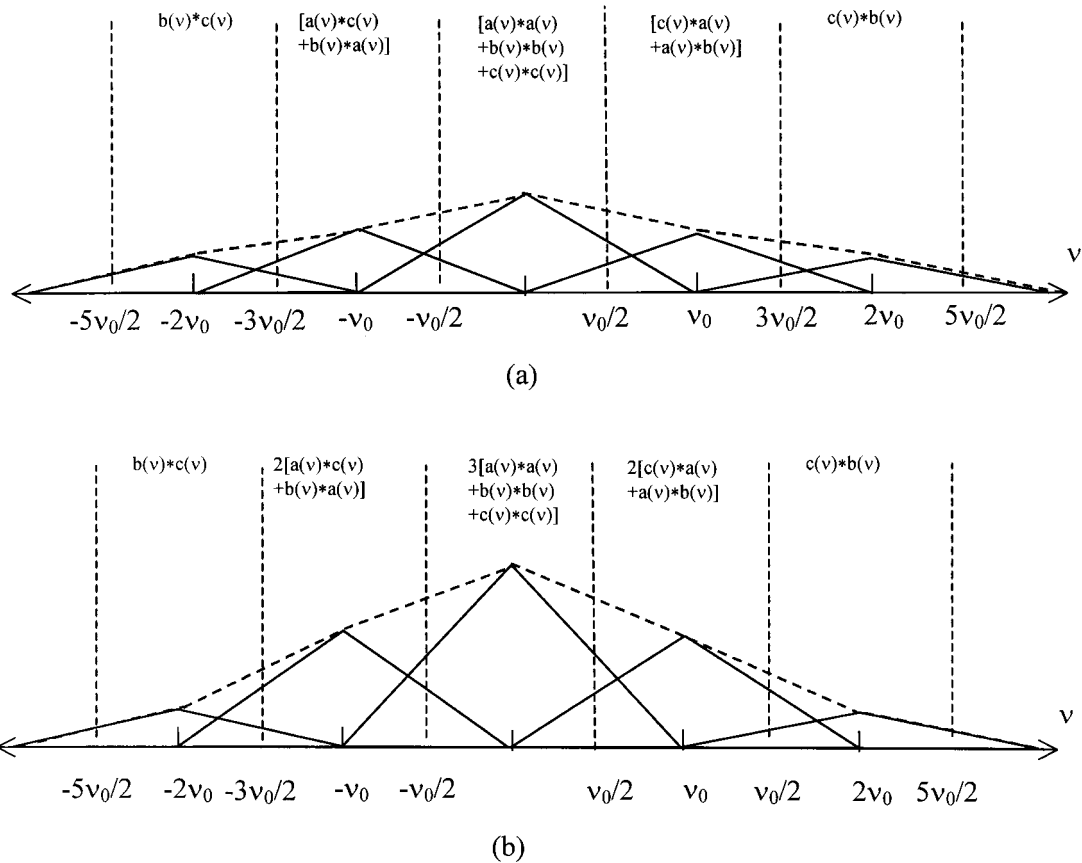


Fig. 3. Spectral intensity after superresolution: (a) Desired output (after time averaging of the field distribution). (b) Superresolved distorted output (after time averaging of the intensity).

the spatial domain. The field distribution after the first grating can be expressed as

$$\begin{aligned}
 U_{\text{In}}(x)G_1(x - V_1t) &= U_{\text{In}}(x) \sum_{n=-1}^1 A_n \\
 &\quad \times \exp[2\pi in v_0(x - V_1t)] \\
 &= U_1(x, t).
 \end{aligned} \tag{4}$$

This grating $[G_1(x - V_1t)]$ is used for encoding the object's spatial information by a temporal phase and to permit its transmission through the limited aperture placed in the center of the imaging system. After the propagation of light through the first lens, a FT of the field distribution is performed:

$$\begin{aligned}
 \tilde{U}_1(v, t) &= \int U_1(x, t) \exp(-2\pi ivx) dx \\
 &= \sum_{n=-1}^1 A_n \tilde{U}_{\text{In}}(v - nv_0) \exp(-2\pi in v_0 V_1t) \\
 &= \sum_{n=-1}^1 A_n \tilde{U}_{\text{In}}(v - nv_0) \exp(in\phi).
 \end{aligned} \tag{5}$$

Because of the movement of the encoding grating, at the spatial spectrum plane of the system each of the sequential spatial frequency bands is encoded with a different temporal phase ($\phi = -2\pi v_0 Vt$), as can be

seen from Fig. 2(b). The temporal phase can also be interpreted as having a slightly different wavelength (Doppler effect). After a beam passes through the system's finite aperture,

$$\tilde{P}(v) = \text{rect}(v/\Delta v), \tag{6}$$

a low-pass signal is obtained [Fig. 2(c)]:

$$\begin{aligned}
 \tilde{U}_2(v, t) &= \tilde{P}(v) \tilde{U}_1(v, t) \\
 &= [A_{-1}b(v) \exp(-i\phi) + A_0a(v) \\
 &\quad + A_1c(v) \exp(i\phi)].
 \end{aligned} \tag{7}$$

After the beam propagates through the second lens and just before the second (decoding) grating, another Fourier transform is performed:

$$U_2(x, t) = \int \tilde{P}(v) \tilde{U}_1(v, t) \exp(2\pi ivx) dv. \tag{8}$$

Note that, when a Fourier transform instead of the required inverse FT is performed, an inversion of the x axis occurs. In our case, the inversion does not influence the superresolution process.

At that output plane, the encoded signal is decoded (demodulated) with the second moving grating

$[G_2(x - V_2t)]$. Thus the field distribution phasor is as seen in Fig. 2(d):

$$\begin{aligned}
 U_{\text{Out}}(x, t) &= U_2(x, t)G_2(x - V_2t) \\
 &= \sum_m B_m \exp[2\pi i m v_0(x - V_2t)] \sum_n A_n \\
 &\quad \times \int \tilde{P}(v) \tilde{U}_{\text{In}}(v - n v_0) \\
 &\quad \times \exp(-2\pi i n v_0 V_1 t) \exp(2\pi i v x) dv \\
 &= \sum_{m,n} B_m A_n \int \tilde{P}(v) \tilde{U}_{\text{In}}(v - n v_0) \\
 &\quad \times \exp\{2\pi i [x(v m v_0) - (n V_1 \\
 &\quad + m V_2) v_0 t]\} dv. \tag{9}
 \end{aligned}$$

Now for ($V_1 = V_2 = V$) and if time integration is applied to the intensity with a device such as a photodetector or a CCD, it cancels all expressions that contain a time dependence expressed as a phase shift of ($\phi = 2\pi v_0 m V t$) during the integration process. Hence we get the following expression for the intensity [Fig. 3(b)]:

$$\begin{aligned}
 \tilde{U}_{\text{Out}}(v) * \tilde{U}_{\text{Out}}(v) &= [c(v) * b(v)] \otimes \delta(v - 2v_0) \\
 &\quad + 2[a(v) * b(v) + c(v) * a(v)] \\
 &\quad \otimes \delta(v - v_0) + 3[a(v) * a(v) \\
 &\quad + b(v) * b(v) + c(v) * c(v)] \\
 &\quad \otimes \delta(v) + 2[b(v) * a(v) \\
 &\quad + a(v) * c(v)] \otimes \delta(v + v_0) \\
 &\quad + [(b(v) * c(v))] \otimes \delta(v + 2v_0). \tag{10}
 \end{aligned}$$

Note that Eq. (10) differs from Eq. (3), which is the desired result, by factors multiplying each of the frequency bands. Those factors multiply different correlated expressions. Inasmuch as the bandpass of a correlated expression is the sum of the bandpass of each term in the correlation operation, each frequency band contains terms from bands beside it and creates a distortion that cannot be filtered in the output plane unless a change is made in the system. The coefficients of the various terms in Eq. (10) depend on the number of diffraction orders. For a grating that has Q orders, the coefficients will differ starting from Q down to $[Q - (N - 1)]$, where N is the number of spectral bands contained in the input spatial spectrum. Therefore, under the condition that the expanded synthetic aperture be much wider than the spectral bandwidth of the input object ($Q \gg N$), an approximate superresolving output is obtained, because Eq. (10) becomes almost identical to Eq. (3). In the above analysis, Dammann gratings with equal spectral responses were

used, as was done also for the research reported in Ref. 3. One should note that, if Ronchi gratings were used, different frequency bands would pass with different strengths. This of course would distort the output by essentially providing a low-pass enhancement.

3. Image Processing Techniques for Improved Coherent Superresolution

In Section 2 it was shown that the conventional method for coherent superresolution when two physical moving gratings are used causes distortion of the superresolved image.³ The distortion is due to the fact that the detection process averages intensity values rather than field distribution. Shemer *et al.*⁹ have shown that digital processing can replace the second grating with a virtual grating. Furthermore, when the virtual grating is used, the distortion mentioned above no longer exists. A simple explanation for this result can be seen when one looks at the field distribution after the finite aperture, as presented by Eq. (8). This is the field distribution that impinges upon the CCD when no decoding grating is present. The CCD grabs the intensity and transfers it to the computer. The computer processing uses a stored (or generated) intensity grating image and multiplies it by the grabbed image. The result is stored and added to the next image product to produce the desired time averaging. Because multiplication is done between intensity images, no distortion is present when time averaging is performed. In this case, the only distortion that appears in the reconstructed image can result from use of a Ronchi grating instead of a Dammann grating as the encoding (first) grating. However, if a Ronchi grating is used for encoding the input information, compensating techniques (discussed in the following sections) can also be applied to overcome the distortion caused by that grating. This method is flexible but requires a large memory for storing the instantaneous images and a fast CPU for multiplication and to perform the fast FT operations. Therefore, when extensive digital postprocessing cannot be incorporated into an optical system, it is desirable to have methods that can produce accurate coherent superresolution by use of minor digital postprocessing. In what follows, we address this issue and show novel methods for implementing it.

A. Improved Coherent Superresolution Technique That Uses Half-Velocity Movement

The following method is based on using two gratings that are laterally displaced with different velocities. One grating is moving at half the velocity of the other. To understand this concept, let us consider the FT field distribution just after the first grating, as presented by Eq. (5).

The light intensity on the CCD plane after the light passes the second grating is

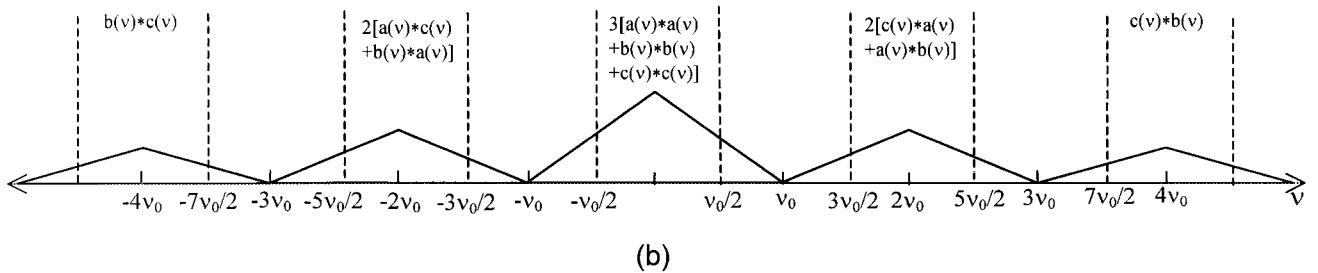
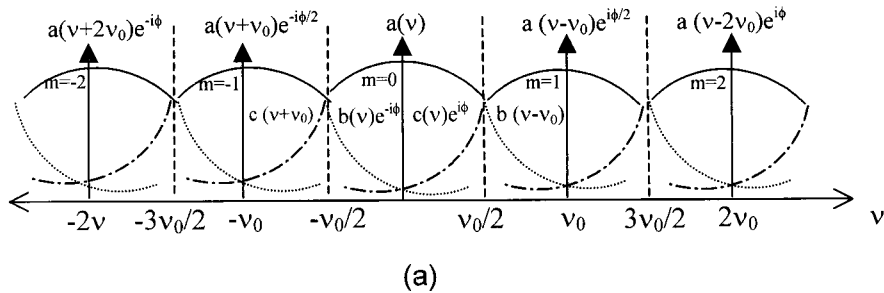


Fig. 4. Half-velocity movement technique: (a) Spectrum of the field distribution after the spectrum passes through the second grating. (It has five orders, and $V_2 = V_1/2$.) (b) Intensity spectrum of (a) after time averaging by the CCD.

$$\begin{aligned}
 I(X, t) &= |U_{\text{Out}}(X, t)|^2 \\
 &= \sum_{m,n} \sum_{m',n'} A_n B_m A_{n'}^* B_{m'}^* \\
 &\times \int \tilde{P}_0(v_1) \tilde{P}_0^*(v_2) \tilde{U}_{\text{In}}(v_1 - n v_0) \tilde{U}_{\text{In}}^*(v_2 \\
 &- n' v_0) \exp[2\pi i [X(v_1 + m v_0 - v_2 - m' v_0) \\
 &- [(m - m') V_2 + (n - n') V_1] v_0 t] dv_1 dv_2.
 \end{aligned} \quad (11)$$

Now, if we move, for example, the second grating with a velocity that is half of the velocity of the first grating, $V_2 = V_1/2$, and time average it with the detector, we get

$$\begin{aligned}
 &\frac{1}{\tau} \int_{-\tau/2}^{\tau/2} \dots \exp[-2\pi i v_0 V_1 t (n - n' \\
 &+ m/2 - m'/2)] dt \\
 &= \begin{cases} 1 & n - n' + 1/2(m - m') = 0 \\ 0 & n - n' + 1/2(m - m') \neq 0 \end{cases}, \quad (12)
 \end{aligned}$$

where

$$\tau = 1/v_0 V_1 = d/V_1 \quad (13)$$

and d is the grating period. By defining the following,

$$\begin{aligned}
 \mu_1 &= v_1 - n v_0, \\
 \mu_2 &= v_2 - n' v_0, \\
 m' &= m + 2n - 2n', \quad (14)
 \end{aligned}$$

and replacing it in the appropriate places in Eq. (11), we obtain

$$\begin{aligned}
 I(X) &= [|U_{\text{Out}}(X)|^2] \\
 &= \sum_m \sum_{m'} B_m B_{m'}^* \iint \left[\sum_n A_n \tilde{P}_0(\mu_1 + n v_0) \tilde{U}_{\text{In}}(\mu_1) \right. \\
 &\times \exp(2\pi i X \mu_1) \exp(-2\pi i X v_0 n) d\mu_1 \\
 &\times \left. \left[\sum_{n'} A_{n'}^* \tilde{P}_0^*(\mu_2 + n' v_0) \tilde{U}_{\text{In}}^*(\mu_2) \right. \right. \\
 &\times \left. \left. \exp(-2\pi i X \mu_2) \exp(2\pi i X v_0 n') d\mu_2 \right] \right]. \quad (15)
 \end{aligned}$$

Here the exponential term $[\exp(2\pi i X v_0 n)]$ in Eq. (15) will cause shifts in the spectral domain as presented schematically in Fig. 4(b) and therefore permit the distorted signal to be corrected. Moreover, the reconstructed image will be obtained only after post-processing, which will realign the spectral regions at the appropriate frequencies in the spectral plane. Furthermore, the decoding grating as shown in Fig. 5

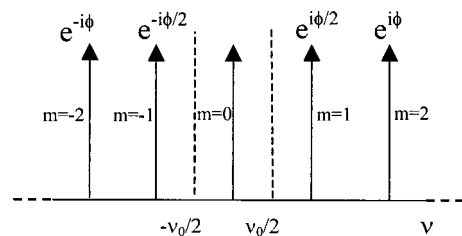


Fig. 5. Slower-moving virtual grating FT as produced in the computer.

has to have twice as many orders for the image to be reconstructed because the odd order, which has a fraction of temporary phase ϕ , is canceled and the remaining terms are related to the even orders of the decoding grating [see Fig. 4(a)]. Hence the spectrum of the reconstructed image before realignment is twice the spectrum of the image after realignment, as can be seen by comparison of Figs. 3(b) and 4(b).

B. Improved Coherent Superresolution Technique That Uses Multiple Gratings

According to Eq. (15) but with $V_1 = V_2$, the intensity obtained in the CCD after time averaging in the detection process and when coherent illumination is used can be expressed as

$$\begin{aligned}
 I(X) &= \text{Mean}|U_{\text{Out}}(X, t)|^2 \\
 &= \sum_m \sum_{m'} B_m B_{m'}^* \iint \left[\sum_n A_n \tilde{P}_0(\mu_1 \right. \\
 &\quad \left. + n\nu_0) \tilde{U}_{\text{In}}(\mu_1) \exp(2\pi i X \mu_1) d\mu_1 \right] \\
 &\quad \times \left[\sum_{n'} A_{n'}^* \tilde{P}_0^*(\mu_2 + n'\nu_0) \tilde{U}_{\text{In}}^*(\mu_2) \right. \\
 &\quad \left. \times \exp(-2\pi i X \mu_2) d\mu_2 \right], \quad (16)
 \end{aligned}$$

where

$$\begin{aligned}
 \mu_1 &= \nu_1 - n\nu_0, \\
 \mu_2 &= \nu_2 - n'\nu_0, \\
 m' &= m + n - n'. \quad (17)
 \end{aligned}$$

To avoid the overlapping exhibited in Fig. 3(b) and to apply correction factors for each band, we consider two approaches: In the first approach the spectrum of the object is used, and in the second approach the system transmission is used. We consider the case in which the first grating is divided into two regions. The first region consists of a grating that has the Fourier coefficients.

$$A_n^{\text{Even}} = \begin{cases} 1 & |n| \leq (N-1)/2 \quad n \text{ even} \\ 0 & |n| > (N-1)/2 \quad \text{otherwise} \end{cases} \quad (18)$$

The second region should consist of a grating that has odd orders. However, because an intensity grating with odd orders and zero dc power is not physical, digital subtraction between the basic grating that has all the orders and the even-order grating must be made:

$$\begin{aligned}
 A_n^{\text{All}} - A_n^{\text{Even}} &= A_n^{\text{Odd}} \\
 &= \begin{cases} 1 & |n| \leq (N-1)/2 \quad n \text{ odd} \\ 0 & |n| > (N-1)/2 \quad \text{otherwise} \end{cases} \quad (19)
 \end{aligned}$$

In this case the Fourier transform of each summation term will be as shown in Fig. 6(a) for the first grating

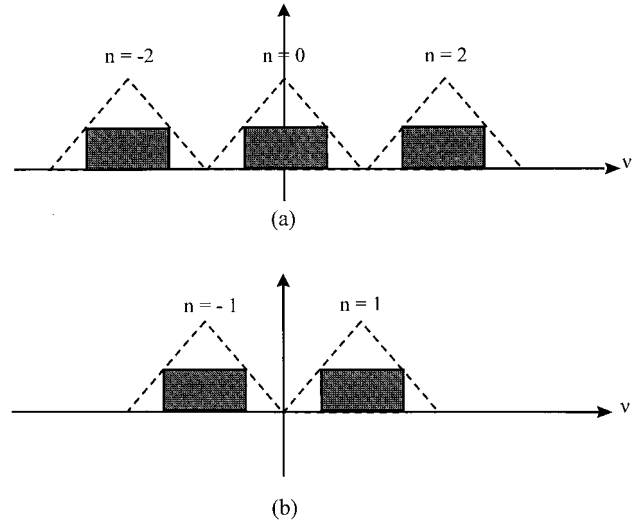


Fig. 6. Multiple-grating approach to superresolution, which yields spectral band separation and nonoverlapping cross correlation terms (dashed lines): (a) even-order grating, (b) odd-order grating.

type and in Fig. 6(b) for the second type. One may see that now, because separate regions exist between the transmission regions, there will be no overlap among the spectral bands because no information will be transmitted. Thus spectral correction may be made by minor postprocessing. After the corrections the output results obtained for each grating type are summed to produce the reconstructed image.

In the second approach we assume that the second grating is also divided into two regions in the same way as in the previous approach. The first region consists of a grating with Fourier coefficients

$$B_m^{\text{Even}} = \begin{cases} 1 & |m| \leq (N-1)/2 \quad m \text{ even} \\ 0 & |m| > (N-1)/2 \quad \text{otherwise} \end{cases} \quad (20)$$

and the second region consists of a basic grating that has all the orders, which, after digital subtraction with the even-order grating, can produce the required odd-order grating:

$$\begin{aligned}
 B_m^{\text{All}} - B_m^{\text{Even}} &= B_m^{\text{Odd}} \\
 &= \begin{cases} 1 & |m| \leq (N-1)/2 \quad m \text{ odd} \\ 0 & |m| > (N-1)/2 \quad \text{otherwise} \end{cases} \quad (21)
 \end{aligned}$$

When the values of m or n are even, the reconstructed image for this region will also contain even spectral parts of the original spectrum, which are related to the even orders of the grating [see Fig. 6(a)]. When m or n is odd, the reconstructed image for this region will contain odd spectral parts, which are related to the odd orders of the grating [see Fig. 6(b)]. Thus the autocorrelation expression $\sum_m B_{m+n-n'} B_{m'}^*$ will have separate regions to prevent overlapping of the spectral bands, and a spectral correction may be made by postprocessing with simple digital elements.

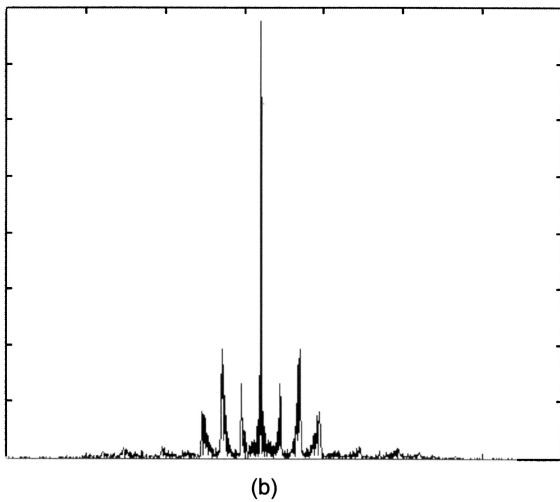
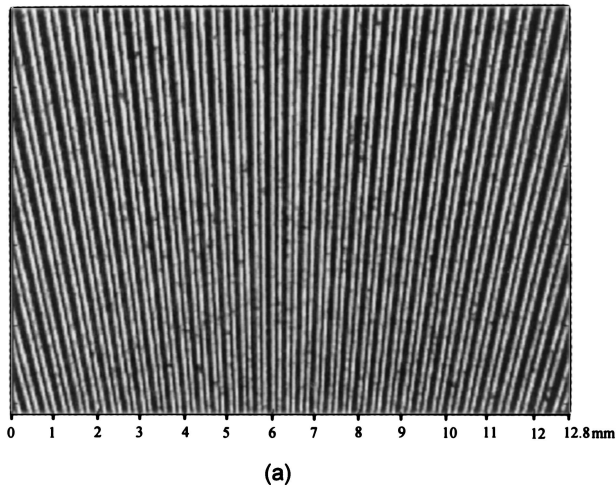


Fig. 7. (a) Input image; (b) horizontal cross section of the input image's spectrum.

After corrections, the output results obtained for each grating type are summed.

4. Experimental Results

To demonstrate the suggested approach, we performed experiments based on the multiple-grating technique. In the experiment we used coherent illumination from a YAG laser with $\lambda = 532$ nm (maximum power, of 500 mW) and, for the input image, a portion of a rosette [Fig. 7(a)]. Each row in the rosette exhibits a different spatial frequency in the horizontal direction, as one can see from the cross section of the one-dimensional Fourier transform [Fig. 7(b)]. This allows us to investigate the superresolving capabilities of different frequencies exhibited in each row. Each of the methods presented in this paper can be implemented and compared with the other methods by use of the virtual grating technique; therefore it was more convenient and more accurate to conduct the experiments with a virtual grating. The setup used for the experiments is the same as shown in Fig. 1. The first

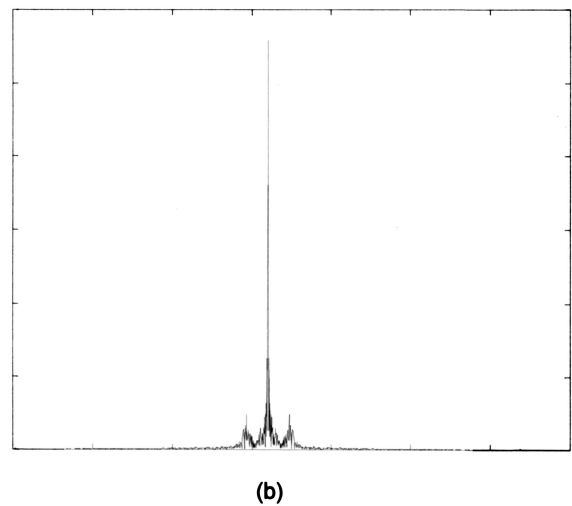
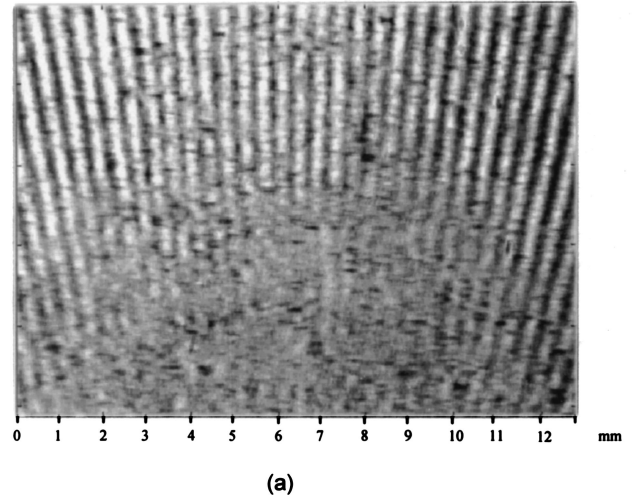
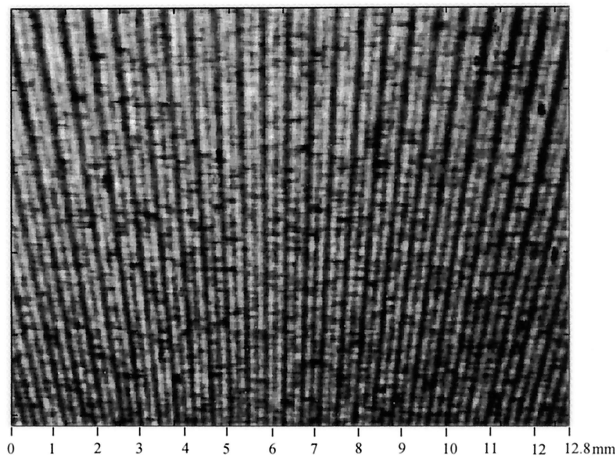
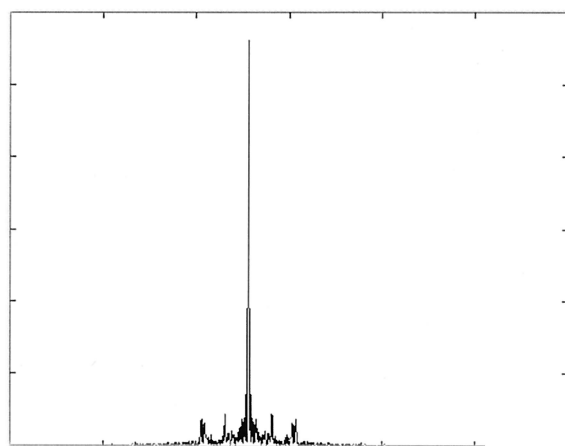


Fig. 8. (a) Distorted input image after the image passes through the system's finite aperture; (b) horizontal cross section of the distorted input image's spectrum.

grating for encoding was a Ronchi grating with a basic period of $100 \mu\text{m}$. This grating was shifted a distance that equals a known fraction of the period; then the image was grabbed and multiplied by a shifted version of the grating in a computer. A slit was placed in the Fourier plane (the aperture plane) to mimic a low-performance imaging system (see Fig. 8). Exploiting the Fourier coefficients of the Ronchi grating should yield at least a $3\times$ improvement in superresolution. Figure 9(a) is the image obtained from the computer decoding superresolution approach without correction for the Ronchi grating distortion. Figure 10(a) presents the same output but with the correction for the Ronchi grating. Note that the only distortion presented here is due to the use of a Ronchi grating. However, the correction shows that other distortions and imperfections suffered by the reconstructed image can be corrected. In all the output images, a cross section of the output spectrum in each case was also presented. It can easily be seen that the corrected



(a)



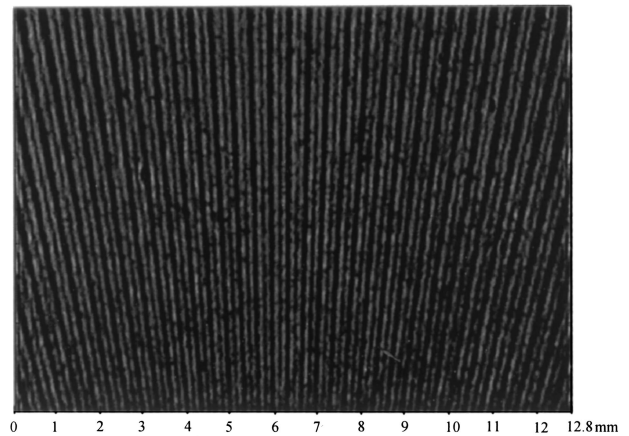
(b)

Fig. 9. Experimental results of the virtual grating method: (a) the reconstructed image without correction; (b) horizontal cross section FT of the reconstructed image without correction.

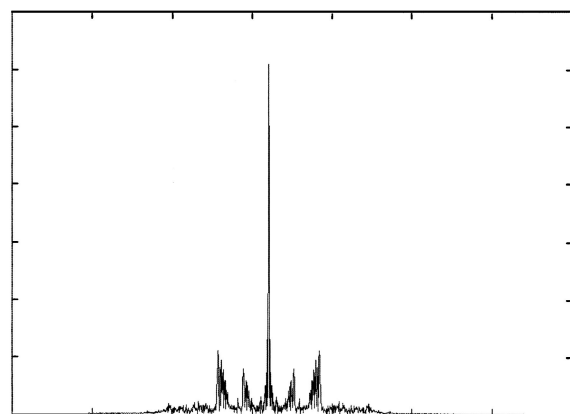
resolved image in Fig. 10 exhibits less distortion than the noncorrected resolved image depicted in Fig. 9.

5. Conclusions

In this paper we have introduced and experimentally demonstrated novel approaches to obtaining improved superresolution under coherent illumination. Our aim has been to overcome the distortions inflicted by the use of coherent illumination and by the use of a Ronchi grating for encoding the information. One method for obtaining superresolution is based on using a virtual grating with correcting factors implemented by a computer. However, the trade-off is the need for massive computer calculations. The other methods are based on two physical gratings and require minor digital calculations. The experimental results show the optoelectronic applications of the proposed techniques.



(a)



(b)

Fig. 10. Experimental results of the multiple-grating approach to obtaining improved superresolution: (a) reconstructed image with correction; (b) horizontal cross section of the spectrum of (a).

The authors acknowledge the help and insight of Carlos Ferreira, which have led to a better understanding of the superresolution concept. Furthermore, this research was partially supported by the Spanish Direccin General de Enseñanza Superior under project PB961134-CO2-02.

References

1. M. Francon, "Amélioration de résolution d'optique," *Nouvo Clemento Suppl.* **9**, 283–290 (1952).
2. W. Lukosz, "Optical systems with resolving powers exceeding the classical limits. II," *J. Opt. Soc. Am.* **57**, 932–941 (1967).
3. D. Mendlovic, A. W. Lohmann, N. Konforti, I. Kiryuschev, and Z. Zalevsky, "One-dimensional superresolution optical system for temporally restricted objects," *Appl. Opt.* **36**, 2353–2359 (1997).
4. A. W. Lohmann and D. P. Paris, "Superresolution for nonbirefringent objects," *Appl. Opt.* **3**, 1037–1043 (1964).
5. A. I. Kartashev, "Optical systems with enhanced resolving power," *Opt. Spectra* **9**, 204–206 (1960).
6. D. Mendlovic and A. W. Lohmann, "Space-bandwidth product adaptation and its application to superresolution: fundamentals," *J. Opt. Soc. Am. A* **14**, 558–562 (1997).

7. D. Mendlovic, A. W. Lohmann, and Z. Zalevsky, "Space-bandwidth product adaptation and its application to superresolution: examples," *J. Opt. Soc. Am. A* **14**, 563–567 (1997).
8. D. Mendlovic, D. Farkas, Z. Zalevsky, and A. W. Lohmann, "High-frequency enhancement by an optical system for super-resolution of temporally restricted objects," *Opt. Lett.* **23**, 801–803 (1998).
9. A. Shemer, D. Mendlovic, Z. Zalavsky, J. Garcia, and P. G. Martinez, "Superresolving optical system with time multiplexing and computer decoding," *Appl. Opt.* **38**, 7245–7251 (1999).